Adsorption of Linear Alkanes in the α-Cages and γ-Cages of H-ZK-5 and K-ZK-5[1]

Willy J. M. van Well,[†] Jochen Jänchen,[‡] Jan W. de Haan,[†] and Rutger A. van Santen*[,†]

Schuit Institute of Catalysis, Laboratory for Inorganic Chemistry and Catalysis, Eindhoven University of Technology, P.O. Box 513, 5600 MB Eindhoven, The Netherlands, and ZeoSys GmbH (Zeolithsysteme), Haus 6.1, Rudower Chaussee 5, 12484 Berlin-Adlershof, Germany

Received: September 29, 1998; In Final Form: December 18, 1998

The adsorption properties of linear alkanes in H-ZK-5 and K-ZK-5 were studied at room temperature by means of sorption and ^{13}C NMR measurements and by molecular simulations. Alkane molecules up to *n*-heptane are able to adsorb in the α- and γ-cages of ZK-5, but adsorption of longer alkane molecules is limited to the large α-cages as a result of size exclusion from the small γ-cages. These γ-cages are the preferred adsorption sites for propane and *n*-butane because of the more favorable heats of adsorption. In contrast, *n*-hexane and *n*-heptane adsorb preferentially in the large α-cages because of the larger entropy in these cages. For *n*-pentane, the γ-cages are the preferred adsorption sites in H-ZK-5, whereas in K-ZK-5 the α-cages are the preferred adsorption sites. This difference is caused by the presence of the potassium cations in the γ-cages of K-ZK-5 which constrains the adsorption in these cages. The difference in siting of molecules with different chain lengths is the result of a steep decrease of the entropy of the adsorbed molecules in the γ-cages with increasing chain length. The ^{13}C NMR measurements and molecular simulations show that the molecules in the γ-cages are in general more coiled than those in the α-cages. Although the conformational equilibria of the molecules in the α-cages of H-ZK-5 and K-ZK-5 are comparable, the molecules in the γ-cages of K-ZK-5 are considerably more coiled than those in the γ-cages of H-ZK-5. The simulation parameters describing the zeolite−alkane interaction were tested by a comparison of the simulation results with the experimental findings.

1. Introduction

Knowledge and understanding of the adsorption properties of zeolites is necessary for the understanding and the prediction of the performance of a zeolite as an adsorbent and as a catalyst. On the one hand, these properties are influenced by the pore topology and chemical composition of the zeolite. On the other hand, they are highly dependent on the properties of the adsorbate itself. The adsorption properties of hydrocarbons are, for example, dependent on the kinetic diameter and on the length of the molecule. Previous studies showed that variation of the chain length can have surprising effects on the adsorption properties as a result of the molecular dimensions of the pores and the cages of zeolites.

The fit between the chain length of *n*-hexane and *n*-heptane molecules and the length of the zigzag channels causes in zeolite silicalite an adsorption and desorption behavior of these molecules that is very different from that of shorter and longer *n*-alkanes.[2−4] This difference is caused by a high degree of ordering of the *n*-hexane and *n*-heptane molecules in the pores of silicalite, leading to a very low entropy of the adsorbed molecules. Furthermore, a change in the distribution of the adsorbed molecules over the zigzag and straight channels of silicalite has been predicted to occur as a function of chain length.[5] Variations in the preferred adsorption sites have also been found for the adsorption of alkanes in ferrierite. Although short molecules such as propane and *n*-butane adsorb easily in the complete pore structure of ferrierite (channels and cages), *n*-hexane and longer molecules are excluded from adsorption in the cages and adsorb only in the channels. The size exclusion of these long molecules is the result of the limited volume of the cages.[6] An interesting intermediate case is *n*-pentane which adsorbs initially only in the channels and for which relatively high pressures are needed to enable adsorption in the cages. This behavior is also due to the limited volume of the cages which leads to a high number of repulsive interactions between *n*-pentane and the oxygen atoms of the zeolite framework, resulting in a relatively low heat of adsorption of *n*-pentane in the ferrierite cages.[7,8]

The examples described above show that the adsorption in zeolites is determined by a subtle interplay of adsorption enthalpy and entropy and that deviations in the adsorption properties can be caused by differences in adsorption enthalpy and/or entropy. We will describe in this study the adsorption properties of linear alkanes in ZK-5. The pore topology of zeolite ZK-5 consists of two types of cages, α- and γ-cages, with different volumes. As a consequence of the difference in volume, differences in both adsorption enthalpy and entropy are expected. These differences may well result in different distributions of the molecules over the two cages as a function of chain length. The pore topology of zeolite ZK-5 is therefore very well suited to the study of adsorption properties of alkanes in zeolites. The cages of ZK-5 are interconnected by narrow eight-ring windows with a diameter comparable to the kinetic diameter of the *n*-alkane molecules. As a consequence, adsorption of *n*-alkane molecules is only possible in the cages and not in the eight-ring windows.[6−9] This means that the ZK-5 pore topology consists of separated cages with limited volumes. The filling of such cages with a range of hydrocarbons has not been studied in detail, despite the large number of zeolite pore structures consisting of such cages. Furthermore, we will investigate the influence of extra-framework cations by comparing the adsorp-

[†] Eindhoven University of Technology.
[‡] ZeoSys GmbH (Zeolithsysteme).

10.1021/jp983905w CCC: $18.00
Published on Web 02/25/1999

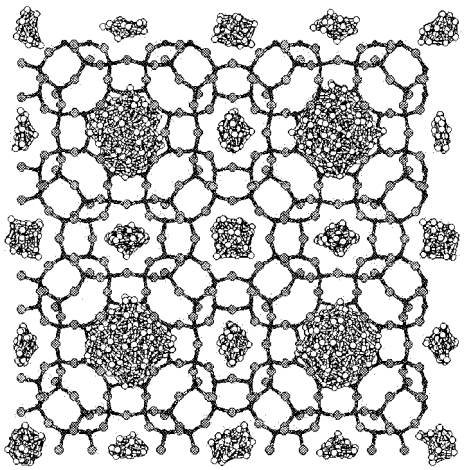

Figure 1. Projection of the cubic ZK-5 structure and the available pore volume showing the large α-cages and small γ-cages.

tion properties, and in particular, the dependence of these properties on the chain length in H-ZK-5 and K-ZK-5.

The adsorption and desorption behavior of the alkane molecules was studied by isotherm and temperature-programmed desorption (TPD) measurements and by molecular simulations. ^{13}C NMR spectroscopy and molecular simulations were used to study the distribution of the molecules over the α- and γ-cages and to study the conformational equilibria of the molecules as a function of chain length and loading. The previous studies on the adsorption of alkanes in silicalite and in ferrierite showed that a combination of sorption, spectroscopic, and simulation methods enabled one to obtain a thorough understanding of the adsorption behavior. Furthermore, a comparison of the simulation results with the experimental results was made to test the simulation parameters describing the zeolite−alkane interaction. These parameters were derived from adsorption data in silicalite and it is important to determine how accurately these parameters predict the adsorption properties of *n*-alkanes in other zeolites. The adsorption in zeolite ZK-5 is a very good test for these parameters because its pore structure is completely different from the channel structure of silicalite. These simulation parameters were tested previously on the adsorption of *n*-alkanes in ferrierite.[8]

1.1. Structure of ZK-5. Zeolite ZK-5 (structure code KFI) was first synthesized by Kerr in 1966; two framework structures isotopic to ZK-5 containing occluded $BaCl_2$ (zeolite P) or $BaBr_2$ (zeolite Q) were synthesized earlier by Barrer.[10,11] The cubic pore structure of zeolite KFI consists of two types of cages interconnected by eight-membered oxygen rings. The largest cage is the α-cage with a free volume of approximately 707 Å^3.[12] The second cage is the so-called γ-cage with a free volume of 264 Å^3.[12] A projection of the cubic ZK-5 structure and the available pore space is given in Figure 1. Every α-cage is connected along the octahedral directions to six γ-cages (one above, one below, and four in the plane of the paper) and every γ-cage is connected to two α-cages (one below and one above, or two in the plane of the paper) and four other γ-cages (one above, one below, and two in the plane of the paper). The α- and γ-cages are connected through flat eight-membered rings with a diameter of 3.9 Å. A puckered eight-membered ring with a smallest diameter of 3.0 Å connects the γ-cages with each other. One unit cell (UC) consists of two α-cages and six γ-cages; this leads to a theoretical pore volume for acidic ZK-5 of 0.305 mL/g.[12]

The positions of the extra-framework potassium cations in K-ZK-5 were studied by Lievens et al.[13] In a sample with a Si/Al-ratio of 3.3 (22 K^+ per unit cell), they found one potassium ion in nearly all puckered eight-membered rings (12 per unit cell). 8−9 K^+ ions were found to be located in the flat eight-membered rings; the remaining cations were located in the hexagonal prisms which connect the α-cages with each other. Significant deformations in the zeolite framework were observed by Parise as a result of ion exchange of (Cs,K)-ZK-5 via its ammonium form to H-ZK-5.[14]

We used zeolite CaA as a "reference" for the α-cages of zeolite ZK-5. The pore structure of CaA consists only of α-cages interconnected through an oxygen eight-membered ring with a diameter of 4.1 Å. Per unit cell, there is one α-cage with a free volume of approximately 811 Å^3.[12] The theoretical pore volume of CaA is 0.285 mL/g.[12]

2. Experimental and Simulation Details

2.1. Materials. The H-ZK-5 samples were prepared by activation of two NH_4-ZK-5 samples obtained from E. I. DuPont de Nemours (Wilmington, DE) with the following compositions: E82122-140-2: $(NH_4)_{20}K_{0.3}Al_{20}Si_{76}O_{192}$ and E34521-73R3A:$(NH_4)_{22}Cs_2K_{0.6}Al_{22}Si_{74}O_{192}$. The first sample was used in the TPD and NMR experiments; the adsorption isotherms were measured on the second sample. As-synthesized zeolite K-ZK-5 (code JP1320) with a Si/Al ratio of 3.3 was provided by Exxon Chemical Europe Inc. (Machelen, Belgium). A small amount of this K-ZK-5 sample was ion exchanged to its ammonium counterpart, and after removal of ammonia, the sample was used in a few TPD experiments. Zeolite CaA was prepared from NaA by ion exchange in a $CaCl_2$ solution with a threefold excess of calcium.

Propane 2.5 (purity 99.5%) and *n*-butane 3.5 (purity 99.95%) were obtained from Hoek Loos (Schiedam, The Netherlands). Propane-1-^{13}C was obtained from Isotec Inc. (Miamisburg, OH). The liquid *n*-alkanes (purity at least 99%) were obtained from Janssen Chimica (Geel, Belgium).

2.2. TPD and Heat of Adsorption Measurement. A Seteram TG-DSC 111 operated under a helium flow of about 3.0 L/h was used in these experiments. The K-ZK-5 samples were activated at 623 K and the CaA samples were activated at 723 K for 10 min. The NH_4-ZK-5 samples had to be activated at 723 K during 10 h to desorb all ammonia. Adsorption was performed at room temperature at a pressure of 20 kPa (propane and *n*-butane) or at relative pressure of 0.2 (liquid *n*-alkanes). Saturation of the sample was checked by observing both the changes in the mass and in the heat flow. The time required to reach saturation varied from 2 to 7 h depending on the sorbate and the zeolite sample. After saturation, the flow with sorbate was switched off and the temperature program was started. A heating rate of 5 K/min was used up to a temperature of 723 K.

The overall heat of adsorption, from zero filling to the maximum loading, was determined at 293 K by means of the above-described adsorption procedure. The heats of adsorption over specific ranges of loading were measured by starting the saturation of the sample from a certain loading obtained by preadsorption.

2.3. Adsorption Isotherm Measurement. The adsorption isotherms were determined gravimetrically at 298 K with a common McBain quartz spring balance equipped with MKS Baratron pressure sensors. Both adsorption and desorption measurements were performed. The sensitivity of the quartz spring amounted to 4 mg/mm. The extension of the spring was measured using a high-precision cathetometer with a resolution of 0.01 mm. Before application, the samples (about 150 mg) were calcined in high vacuum ($<10^{-6}$ kPa) at 673 K for 4 h.

TABLE 1: Size and Energy Parameters of the Different Used Parameter Sets Describing the Interaction between the Framework Oxygen Atoms and the Alkane United Atoms

parameter set	$\sigma_{CH3,O} = \sigma_{CH2,O}$ [Å]	$\epsilon_{CH3,O}$ [K]	$\epsilon_{CH2,O}$ [K]
propane	3.636	73.4	73.4
Smit et al.	3.64	87.5	54.4
June et al.	3.364	83.8	83.8

The adsorption isotherms of *n*-pentane, *n*-hexane, and *n*-heptane on H-ZK-5 and K-ZK-5 were measured. The time required to reach equilibration was strongly dependent on the loading, and the adsorbate. Equilibration was reached within 1 h for *n*-pentane at high loadings, whereas the equilibration time was at least 2 h for *n*-heptane. At low loadings, equilibration took place overnight.

2.4. ^{13}C Cross-Polarized Magic Angle Spinning (CP MAS) NMR Measurement. The closed glass capsules containing the zeolite sample (15−30 mg) and the adsorbed alkane molecules were prepared as described previously.[7] The zeolites were activated overnight by evacuation ($p < 10^{-4}$ kPa) and heating to the required dehydration temperature (723 K for CaA and NH_4-ZK-5, 623 K for K-ZK-5). The ^{13}C CP MAS NMR measurements were performed on a Bruker MSL 400 at 9.4 T at room temperature. The capsules were placed in a 7 mm MAS rotor and spun at a rate of 2500 Hz. The contact time for cross polarization was 10 ms and the repetition delay was 5 s. Several samples were measured also at contact times of 1 and 15 ms to verify the results obtained at 10 ms. Different numbers of scans were accumulated depending on the amount of sample and on the loading of alkane on the sample. Adamantane was used as an external reference to transfer chemical shifts to the δ-scale. The free induction decays (fids) were weighted with a line broadening of 30 Hz prior to Fourier transformation; the resulting spectra were simulated using the WINFIT program of Bruker.

2.5. Simulation Details. The configurational bias−Monte Carlo (CB−MC) simulation method as developed by Smit and Siepmann the computational efficiency of which was improved recently) was used in the grand-canonical ensemble (fixed chemical potential, temperature, and volume) to calculate adsorption isotherms. A detailed description of the method appears elsewhere.[15−19]

The simulations were performed in equilibration and production cycles. Each cycle consists of attempts to perform the various Monte Carlo moves (translation, rotation, and a partial regrowth of a molecule, and an exchange of a molecule with the ideal gas reservoir). The probabilities that one of these moves will be attempted are equal to those used in ref 8.

The alkane molecules are modeled using the united atom model. This means that CH_3 and CH_2 units are treated as single interaction centers. In this model, a constant bond length is used, the bond bending is described by a harmonic potential, the torsional angles are modeled by the Jorgensen potential, and the interactions between the different pseudo-atoms are described by a 12-6 Lennard-Jones potential. Further details on the alkane models are given for propane in ref 20 and for *n*-butane and longer *n*-alkanes in ref 15.

The KFI structure determined by Parise and co-workers on a D-ZK-5 sample was used in the simulations.[14] This structure was kept rigid and all aluminum atoms were replaced by silicon atoms because only the dispersive and repulsive interactions between the alkane molecules and the zeolite framework were taken into account. In the following we denote this all-silica structure as *KFI*. The simulation box used consists of eight unit cells (two in each direction) and its size is consequently 37.346 Å in each direction. Periodic boundary conditions were imposed during the simulations.

TABLE 2: Maximum Loadings in mmol/g and in mol/UC, Occupied Pore Volumes (PV), Temperatures of Mass Loss Maxima, and Amount Desorbed in Second Desorption Stage of *n*-Alkanes in CaA

	loading [mmol/g]	loading [mol/UC]	PV [ml/g]	*T*1 [K]	*T*2 [K]	loading second stage [mol/UC]
C3	–	–	–	–	–	–
nC4	2.1	4.0	0.21		381	
nC5	2.0	3.8	0.23		435	
nC6	1.6	3.1	0.21	387	483	1.8
nC7	1.6	3.0	0.23	375	517	1.9
nC8	1.5	2.9	0.24	331	518	2.1

The dispersive interactions between the zeolite framework and the alkane molecules were described by a 12-6 Lennard-Jones potential between the oxygen atoms of the framework and the united atoms of the alkane chains:

$$U_{LJ} = 4\epsilon_{ij}[(\sigma_{ij}/r_{ij})^{12} - (\sigma_{ij}/r_{ij})^{6}]$$

The size (σ) and energy (ϵ) parameters of this potential were derived from experimental adsorption data on silicalite by both Smit et al.[15,20] and June et al.[21] The two parameter sets, for propane and for *n*-butane and longer *n*-alkanes, derived by Smit et al. are displayed in Table 1 and denoted as propane and Smit et al., respectively. The parameter set derived by June et al. is also displayed in Table 1 and denoted as June et al. parameter set.

The isosteric heat of adsorption was calculated as a function of loading as described previously.[8] A differentiation of the adsorbed molecules was made between molecules located in the α-cage and in the γ-cage based on the coordinates of the central carbon atom of the chain. Finally, the conformational equilibria of the molecules adsorbed in the two different cages was determined.

3. Results and Discussion

3.1. TPD. The occupied pore volumes and maximum loadings of the different alkanes in CaA at 293 K are given in Table 2. The pore volumes are calculated with the density of the liquid alkanes at 293 K relative to water at 277 K. The results show that the maximum number of molecules adsorbed in an α-cage in CaA is four for *n*-pentane and shorter *n*-alkanes, and three for *n*-hexane, *n*-heptane, and *n*-octane. These maximum numbers can be considered as upper limits for adsorption in the α-cages of KFI because the latter have a somewhat smaller free volume than the α-cages in CaA. Table 2 compiles the temperatures of the desorption rate maximum and the number of molecules that desorb in the high-temperature stage. Whereas *n*-butane and *n*-pentane display a single-stage desorption from CaA, the longer molecules desorb in two stages. Two molecules per α-cage desorb in the high-temperature stage and one *n*-hexane, *n*-heptane or *n*-octane molecule per α-cage desorbs in the low-temperature stage. This means that the third molecule per α-cage desorbs much easier than the first two molecules.

The results of the adsorption and the desorption experiments on H-ZK-5 and K-ZK-5 are summarized in Tables 3 and 4, respectively. The crystallinity of the H-ZK-5 sample was checked by measuring the pore volume occupied by methanol. The measured value of 0.27 mL/g compares very well with the values reported by Abrams and Corbin and is only 10% smaller than the theoretical pore volume.[12] The results displayed in Table 3 show that the pore volume occupied by *n*-octane is much

TABLE 3: Maximum Loadings in mmol/g and mol/UC, Occupied Pore Volumes (PV), Temperatures of Mass Loss Maxima, and Amount Desorbed in Second Desorption Stage of *n*-Alkanes in H-ZK-5

	loading [mmol/g]	loading [mol/UC]	PV [ml/g]	*T*1 [K]	*T*2 [K]	loading second stage [mol/UC]
C3	1.7	10.0	0.15		350	
nC4	1.4	8.1	0.14		371	
nC5	1.5	8.8	0.18		385	
nC6	1.7	9.6	0.22	352		
nC7	1.4	8.2	0.21	317	399	3.7
nC8	0.67	3.8	0.11		465	

TABLE 4: Maximum Loadings in mmol/g and mol/UC, Occupied Pore Volumes (PV), Temperatures of Mass Loss Maxima, and Amount Desorbed in Second Desorption Stage of *n*-Alkanes in K-ZK-5

	loading [mmol/g]	loading [mol/UC]	PV [ml/g]	*T*1 [K]	*T*2 [K]	loading second stage [mol/UC]
C3	1.7	11.1	0.15		361	
nC4	1.7	11.0	0.17		385	
nC5	1.5	10.2	0.18	356	410	
nC6	1.5	9.6	0.19	315	425	3.6
nC7	0.75	5.0	0.11	296	431	3.8
nC8	0.61	4.0	0.097		420	

smaller than the pore volumes occupied by the shorter molecules. This indicates that *n*-octane is not able to adsorb in the complete pore structure at the prevailing experimental conditions. The difference between the pore volume occupied by *n*-octane and that occupied by shorter molecules is probably caused by the presence of γ-cages in H-ZK-5 because such a large difference is absent for CaA. Thus, adsorption in the γ-cage appears to be possible only for molecules smaller than *n*-octane. This size exclusion of *n*-octane from the γ-cages is similar to the exclusion of *n*-hexane and longer molecules from the cages of ferrierite.[6−8] Adsorption of the shorter molecules in the γ-cages is indicated because their loadings are too high to be attributed to adsorption in the α-cages only (considering the maximum number of molecules per α-cage obtained for CaA and the presence of two α-cages per KFI unit cell). Adsorption in the γ-cages is probably limited to one molecule per cage because the volume of this cage is less than twice the volume of a propane molecule (148 Å^3, based on the liquid density). This means that the total number of molecules located in the γ-cages is at most six per unit cell. The loadings of *n*-alkanes from propane to *n*-heptane should, therefore, be attributed to adsorption in both types of cages of H-ZK-5. Furthermore, it is interesting to note that the volume of the γ-cages lies between the volumes calculated for the *n*-heptane and *n*-octane molecules (243 and 269 Å^3).

The results of the TPD measurements from H-ZK-5 are depicted in Figures 2 and 3. Figure 2 shows the residual amount of adsorbed alkane as a function of temperature. The differential mass loss curves ($-$d*m*/d*T*) derived from the desorption profiles are displayed in Figure 3. The curve of propane is similar to that of *n*-butane and *n*-pentane and is therefore not displayed. The curves are separated from each other for the sake of clarity. The temperature of the desorption rate maximum and the amount desorbed in the high-temperature stage are given in Table 3.

Figure 2 shows the high maximum loading of *n*-hexane and *n*-heptane; Figures 2 and 3 show that a part of the *n*-hexane and *n*-heptane molecules desorbs at relatively low temperatures. The latter results in a pronounced two-stage desorption profile for *n*-heptane and in a single desorption peak at a very low temperature for *n*-hexane. The occurrence of desorption at low temperatures indicates that at a loading of 9.6 and 8.2 mol/UC,

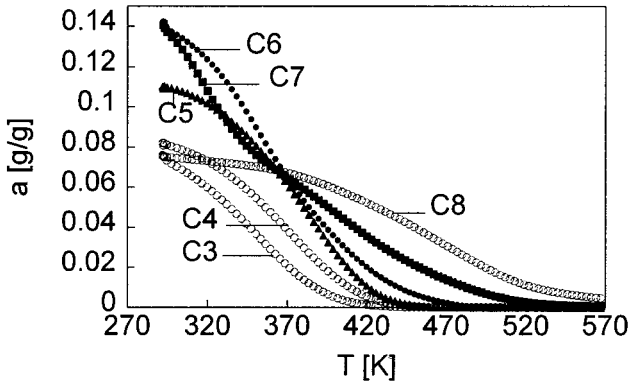

Figure 2. TPD curves of linear alkanes from H-ZK-5.

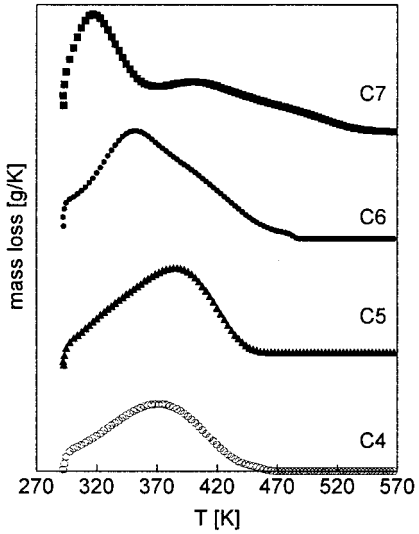

Figure 3. Differential mass loss ($-$d*m*/d*T*) of alkanes during TPD from H-ZK-5.

respectively, a part of the adsorbed *n*-hexane and *n*-heptane molecules has a high (or small negative) Gibbs free energy. According to Table 3, 4.5 mol/UC of *n*-heptane desorbs in the low-temperature stage and 3.7 mol/UC desorbs in the high-temperature stage. Because the desorption profile of *n*-heptane is parallel to that of *n*-octane at high temperatures, it seems reasonable to assume that the second stage is mainly caused by desorption of *n*-heptane from the α-cages. This means that the molecules adsorbed in the γ-cages desorb mainly in the first stage. It is not clear whether desorption from the α-cages, like that observed for CaA, contributes to this first stage.

The maximum loadings achieved in K-ZK-5 are shown in Table 4; an occupied pore volume of 0.18 mL/g was found for methanol. The results displayed in Table 4 reveal that, in contrast to H-ZK-5, a relatively small occupied pore volume was found for *n*-heptane and *n*-octane. However, the pore volume occupied by *n*-heptane was still significantly larger than that of *n*-octane, indicating that *n*-heptane exploits more of the pore structure than does *n*-octane. The maximum loadings of the shorter molecules in K-ZK-5 indicate that these molecules are distributed over the α- and γ-cages, as in H-ZK-5. The desorption profiles of propane to *n*-octane and the differential mass loss curves of *n*-butane to *n*-octane are depicted in Figures 4 and 5, respectively. The pronounced two-stage desorption profile of *n*-pentane from the extra-framework cations containing K-ZK-5 stands in sharp contrast to the results for H-ZK-5. *n*-Hexane and *n*-heptane also desorb in two stages from K-ZK-5. The second desorption stage of these molecules corresponds to the desorption of ca. 3.7 mol/UC from the α-cages (2 mol/α-cage).

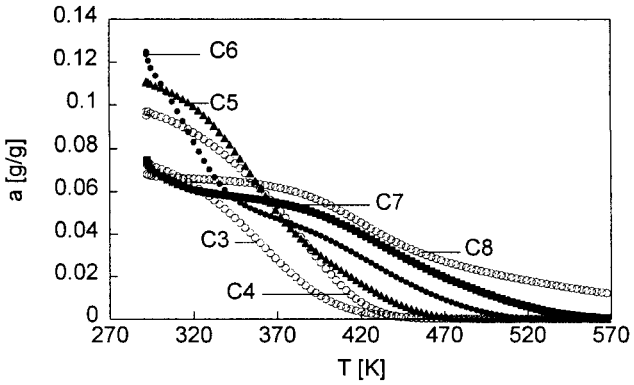

Figure 4. TPD curves of linear alkanes from K-ZK-5.

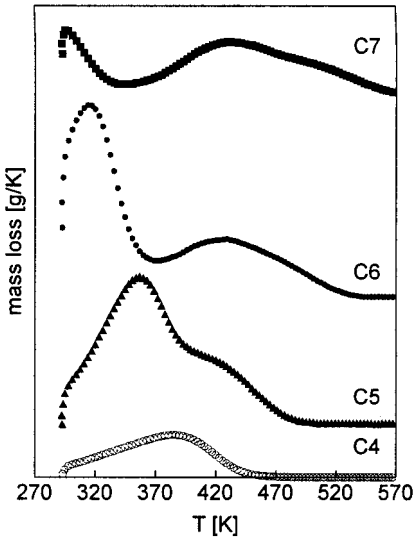

Figure 5. Differential mass loss (−d*m*/d*T*) of alkanes during TPD from K-ZK-5.

Note that a small amount of the K-ZK-5 sample was ion-exchanged to the ammonium form and activated to yield H-ZK-5. This sample was used in a different experimental setup to measure the desorption profiles of *n*-pentane, *n*-hexane, and *n*-heptane. The loadings and desorption profiles measured in these experiments are comparable to the results reported here for H-ZK-5.

It is remarkable and important that the temperatures at which the low-temperature peaks occur decrease with increasing chain length. This stands in contrast to the high-temperature desorption peaks which are ordered according to the chain length of the molecule. The latter is the usual order when desorption of the different alkane molecules is determined by an increase (more negative) of the heat of adsorption with increasing chain length. The different order of the low-temperature peaks shows that desorption at relatively low temperatures (or high loadings) is not determined by an increase of the heat of adsorption with increasing chain length. This desorption behavior at low temperatures is found for all three zeolites CaA, H-ZK-5, and K-ZK-5.

3.2. Adsorption Isotherm Measurement. The adsorption isotherms of *n*-pentane, *n*-hexane, and *n*-heptane on H-ZK-5 and on K-ZK-5 at 298 K are depicted in Figures 6 and 7, respectively. The figures display both adsorption and desorption measurements. The loadings of the *n*-alkanes are expressed in number of molecules per unit cell. For both zeolites, the number of adsorbed molecules increases with chain length at low pressures. Because of the step in the adsorption isotherm of

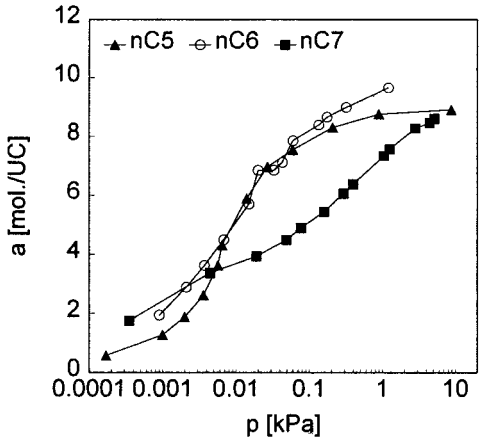

Figure 6. Adsorption isotherms of *n*-pentane, *n*-hexane, and *n*-heptane on H-ZK-5 at 298 K.

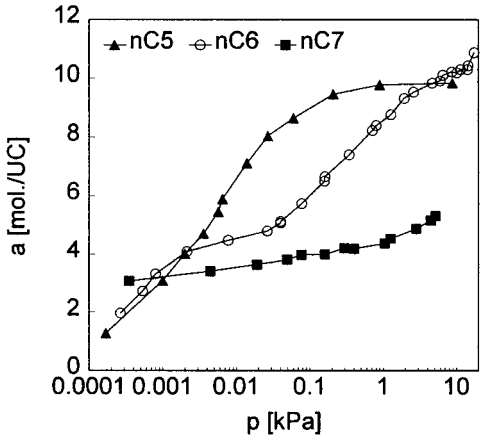

Figure 7. Adsorption isotherms of *n*-pentane, *n*-hexane, and *n*-heptane on K-ZK-5 at 298 K.

n-hexane and the very flat isotherm measured for *n*-heptane on K-ZK-5, the number of adsorbed molecules decreases with increasing chain length at high pressures. For H-ZK-5, the number of molecules adsorbed is approximately equal for *n*-pentane and *n*-hexane, whereas the number of adsorbed *n*-heptane molecules is significantly lower at high pressures. These observations at low and high pressures are comparable to the results of the TPD experiments at high and low temperatures, respectively. The relatively high pressures required to obtain high loadings of the long molecules show that these loadings lead to a relatively high (or small negative) Gibbs free energy of the adsorbed molecules. The pressure required to obtain these high loadings (and thus free energy) is higher when the molecule is longer. This is in agreement with the order at which the low-temperature desorption peaks occur.

The loading at which the steps occur in the isotherms, about 4 mol/UC, corresponds reasonably with the amount of *n*-heptane from H-ZK-5 and the amount of *n*-hexane from K-ZK-5 that desorbs in the high-temperature stage. The small increase of the loading of *n*-heptane on K-ZK-5 at pressures above 1 kPa corresponds to desorption of about 1.2 mol/UC at very low temperatures.

3.3. Heat of Adsorption Measurements. The heats of adsorption of propane to *n*-hexane were measured as a function of loading on a H-ZK-5 sample with a Si/Al ratio of 4 by Eder et al. at 348 K.[22] Although a decrease of the heat of adsorption (heat of adsorption became less negative) with loading was measured for propane, hardly any variation was found for *n*-butane. The heats of adsorption of *n*-pentane and *n*-hexane

TABLE 5: Isosteric Heat of Adsorption ($-q_{st}$) at Different Ranges of Loading (in mol/UC) of *n*-Alkanes on H-ZK-5 and K-ZK-5 at 293 K

nC7/H-ZK-5		nC5/K-ZK-5		nC6/K-ZK-5	
loading [mmol/UC]	$-q_{st}$ [kJ/mol]	loading [mol/UC]	$-q_{st}$ [kJ/mol]	loading [mol/UC]	$-q_{st}$ [kJ/mol]
0−6.8	81	0−10.5	77	0−10.1	85
2.6−6.8	83	5.0−10.5	81	4.3−10.1	85
3.9−6.8	85			5.5−10.1	83

TABLE 6: ^{13}C NMR Chemical Shifts of Propane and Propane-1-^{13}C in K-ZK-5 (K-KFI), H-ZK-5 (H-KFI), and CaA (LTA); Results for Propane-1-^{13}C in K-KFI are Differentiated to Propane in the α-Cages and in the γ-Cages

zeolite	loading	peak I	peak II
K-KFI	8.6	15.9	16.5
K-KFI	4.8	15.6	16.4
K-KFI	2.6	15.4	16.4
		δ (C1/C3) α-cage	δ (C1/C3) γ-cage
K-KFI propane-1-^{13}C	8.6	15.6	16.3
K-KFI propane-1-^{13}C	5.2	15.8	16.4
K-KFI propane-1-^{13}C	3.3		16.4
		peak I	
H-KFI	5.1	15.9	
H-KFI	1.2	16.0	
H-KFI propane-1-^{13}C	4.7	15.8	
		δ (C1/C3) α-cage	δ (C2) α-cage
LTA	2.8	15.7	16.3
LTA	0.9	15.0	15.9
LTA propane-1-^{13}C	2.1	15.2	

increased continuously up to the highest loading measured of approximately 7.4 mol/UC.

We measured the isosteric heat of adsorption of *n*-heptane on H-ZK-5 and *n*-pentane and *n*-hexane on K-ZK-5 at different ranges of loading at 293 K. The results are displayed in Table 5 and show that the heats of adsorption of *n*-heptane on H-ZK-5 and of *n*-pentane on K-ZK-5 increase with loading. A small decrease with loading occurs in the heat of adsorption of *n*-hexane on K-ZK-5 at higher loadings.

The above results show that the heats of adsorption increase with chain length for all molecules and for all loadings. This means that the relatively high (or small negative) Gibbs free energies of the adsorbed longer molecules are due to a low entropy of these molecules at high loadings. The order of the low-temperature desorption peaks and the order of the number of adsorbed molecules at high pressures indicate that the increased loss of entropy with chain length is dominant over the increased gain of enthalpy with chain length.

3.4. ^{13}C CP MAS NMR. *3.4.1. Introduction.* We used ^{13}C NMR spectroscopy to obtain direct information on the distribution of the different molecules over the α- and γ-cages. ^{13}C NMR is a suitable technique for this because the chemical shift of a carbon nucleus depends on the medium (or environment) of the molecule and on the conformational equilibrium of the *n*-alkane molecule. These dependencies of the carbon chemical shift were used previously to study the distribution of alkane molecules over the channels and cages of zeolite ferrierite.[7] A detailed description of the use of ^{13}C NMR spectroscopy for these properties is given in ref 7.

When we compare the carbon chemical shifts of *n*-alkane molecules adsorbed in the α- and γ-cages of ZK-5, the effect of the medium and that of the conformational equilibrium will lead to opposing changes in the chemical shift. On the one hand, adsorption in the smaller γ-cages will lead to larger chemical shifts as a result of medium effects.[23] On the other hand, the *n*-alkane molecules located in these γ-cages will most probably be more coiled than the molecules in the α-cages, which will lead to smaller chemical shifts.[24,25] The effects of the medium and of the conformational equilibria were also opposite in our previous comparison of *n*-alkane molecules adsorbed in the cages and channels of ferrierite.[7] In that study the medium effect (for *n*-butane) was as strong as or stronger (for *n*-pentane) than the effect of the conformational equilibrium for the methyl carbon atoms. Because of the smaller effect of the medium on the methylene carbon chemical shift, the effect of the conformational equilibria was dominant for the methylene carbon atoms of *n*-butane and *n*-pentane.

TABLE 7: ^{13}C NMR Chemical Shifts of *n*-Butane in K-ZK-5 (K-KFI), H-ZK-5 (H-KFI), and CaA (LTA); Results for *n*-Butane in K-KFI are Differentiated to *n*-Butane in the α-Cages and γ-Cages

			δ (C2/C3)	
zeolite	loading	δ (C1/C4)	α-cage	γ-cage
K-KFI	7.3	13.4	25.2	23.9
K-KFI	4.0	13.2	24.9	23.9
K-KFI	2.0	13.1	24.9	23.9
		δ (C1/C4)	δ (C2/C3)	
H-KFI	6.9	13.2	24.9	
H-KFI	1.9	13.2	24.6	
LTA	3.0	13.8	25.5	
LTA	1.2	12.9	25.0	

TABLE 8: ^{13}C NMR Chemical Shifts of *n*-Pentane in K-ZK-5 (K-KFI), H-ZK-5 (H-KFI), and CaA (LTA); Results for *n*-Pentane in K-KFI and H-KFI are Differentiated to *n*-Pentane in the α-Cages and in the γ-Cages

		δ (C1/C5)		δ (C2/C4)		δ (C3)	
zeolite	loading	α-cage	γ-cage	α-cage	γ-cage	α-cage	γ-cage
K-KFI	9.9	14.0	14.7	23.2	19.3	35.9	31.4
K-KFI	6.3	14.3		22.8	19.6	35.4	32.0
K-KFI	3.8	14.1		22.9	19.6	35.8	
K-KFI	2.5	14.0		22.9		35.4	
H-KFI	8.1	14.0	14.8	23.2	21.2	35.0	33.8
H-KFI	5.2	13.5	14.5	22.4	21.1	34.5	33.6
H-KFI	3.3	13.7	14.6	22.3	21.2	34.5	33.7
H-KFI	1.7	13.6	14.5	22.1	21.2	34.2	33.6
LTA	2.6	14.1		23.1		35.0	
LTA	0.9	13.0		22.6		34.6	

We prepared H-ZK-5 and K-ZK-5 samples with different loadings of propane to *n*-heptane to study the influences of alkane chain length and alkane loading on the distribution of the molecules over the α- and γ-cages. CaA samples with different loadings of alkanes from propane to *n*-heptane were used as references for adsorption in the α-cages of ZK-5. Figures 8−13 depict the NMR spectra of propane to *n*-heptane adsorbed in CaA, H-ZK-5 and K-ZK-5 at different loadings; the chemical shifts are given in Tables 6−10.

The ^{13}C CP MAS NMR spectra obtained for alkanes in CaA show that the carbon chemical shifts of molecules adsorbed in the α-cages depend on the loading. An increase of the loading in the α-cage leads for all adsorbates to an increase in the chemical shifts. Because this change is also observed for propane, it is, at least partly, caused by a change in the medium effects experienced by the molecules with increasing loading. The chemical shifts for propane in CaA are smaller than 17 ppm, which is the chemical shift measured for propane adsorbed

TABLE 9: ^{13}C NMR Chemical Shifts of *n*-Hexane in K-ZK-5 (K-KFI), H-ZK-5 (H-KFI), and CaA (LTA); Results for *n*-Hexane in K-KFI and H-KFI are Differentiated to *n*-Hexane in the α-Cages and in the γ-Cages

		δ (C1/C5)		δ (C2/C4)		δ (C3)	
zeolite	loading	α-cage	γ-cage	α-cage	γ-cage	α-cage	γ-cage
K-KFI	9.1	13.6	14.5	23.4	18.4	31.4	25.4
K-KFI	7.3	13.6	14.4	23.0	18.7	31.7	
K-KFI	4.8	13.8		22.8		31.6	
K-KFI	2.9	13.7		23.0		31.9	
H-KFI	8.5	14.4	14.4	23.4	20.9	32.8	28.5
H-KFI	5.1	13.8		22.8	21.1	31.8	28.6
H-KFI	3.0	13.4	14.2	22.6	20.9	31.6	28.5
H-KFI	1.8	13.3		22.6		31.4	
LTA	2.5	13.7		23.5		32.7	
LTA	0.8	12.8		22.7		31.7	

TABLE 10: ^{13}C NMR Chemical Shifts of *n*-Heptane in K-ZK-5 (K-KFI), H-ZK-5 (H-KFI), and CaA (LTA); Results for *n*-Heptane in K-KFI and H-KFI are Differentiated to *n*-Heptane in the α-Cages and in the γ-Cages

		δ (C1/C7)		δ (C2/C6)		δ (C3)	
zeolite	loading	α-cage	γ-cage	α-cage	γ-cage	δ (C3/C5)	δ (C4)
K-KFI	4.9	13.8		22.3	18.5	31.5 & 25.1	28.1
K-KFI	4.2	13.8		22.2		31.4	28.1
K-KFI	2.3	13.8		22.7		31.7	28.0
H-KFI	7.3	14.5	14.5	22.8	20.9	32.4	28.6
H-KFI	5.4	13.7	14.4	22.8	20.9	31.4	28.4
H-KFI	3.4	13.4	14.2	22.2	20.8	31.3	28.2
H-KFI	2.1	13.3	14.3	22.1	20.9	31.2	27.9
LTA	2.3	14.2		23.0 & 23.8		33.0	29.7
LTA	1.1	13.0		22.1 & 22.8		31.6	28.4

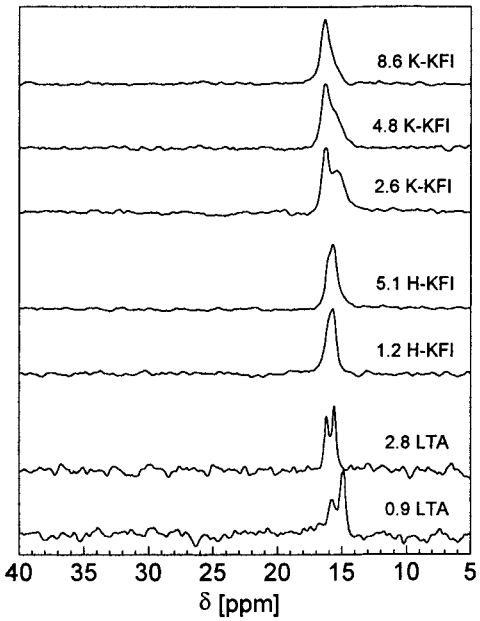

Figure 8. ^{13}C NMR spectra of propane in K-ZK-5 (K-KFI), H-ZK-5 (H-KFI), and CaA (LTA) at different loadings, indicated in units of molecules per unit cell.

in the cages of ferrierite.[7] This is as expected because the ferrierite cages have a smaller free volume than do the α-cages of zeolite A.

3.4.2. Distributions of the Molecules. The spectra of propane adsorbed in CaA, H-ZK-5, and K-ZK-5 are depicted in Figure 8. The methyl and methylene signals are clearly separated in the CaA spectra. Only one peak is found for propane adsorbed in H-ZK-5, whereas adsorption of propane in K-ZK-5 results in two signals. The spectra of propane-1-^{13}C are displayed in

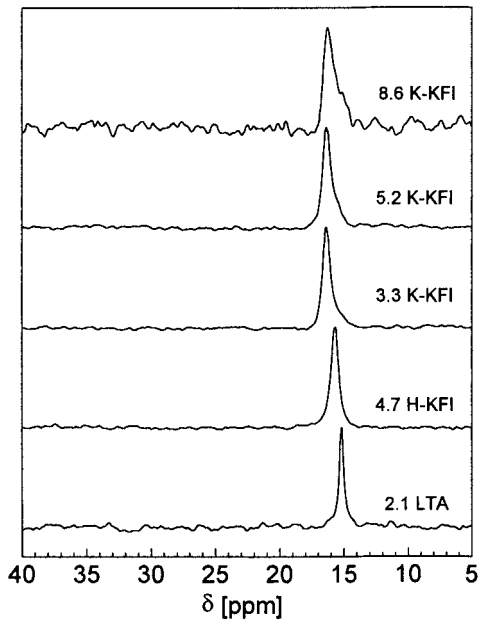

Figure 9. ^{13}C NMR spectra of propane-1-^{13}C in K-ZK-5 (K-KFI), H-ZK-5 (H-KFI), and CaA (LTA) at different loadings, indicated in units of molecules per unit cell.

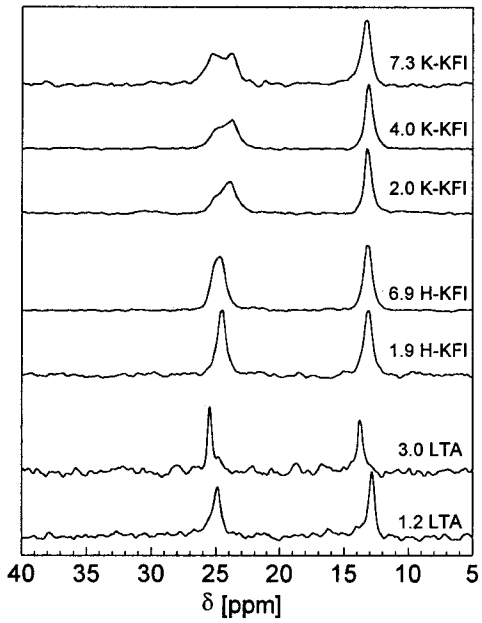

Figure 10. ^{13}C NMR spectra of *n*-butane in K-ZK-5 (K-KFI), H-ZK-5 (H-KFI), and CaA (LTA) at different loadings, indicated in units of molecules per unit cell.

Figure 9. The chemical shift of the methyl peak increases from CaA via H-ZK-5 to K-ZK-5. The shift of 16.4 ppm measured for K-ZK-5 at low loadings is 1.2 ppm larger than the value measured for CaA and indicates, therefore, that propane adsorbs preferentially in the γ-cages of K-ZK-5. At higher loadings, a shoulder occurs around 15.7 ppm indicating adsorption in the α-cages. This result means that the peak at 15.5 ppm of unlabeled propane in K-ZK-5 represents the methylene carbon atom of propane in the γ-cages. The signal of propane in H-ZK-5 is situated exactly between the signal of CaA and that of the γ-cage of K-ZK-5 and is, therefore, not assigned.

Figure 10 shows the spectra of *n*-butane adsorbed in CaA, H-ZK-5, and K-ZK-5. For K-ZK-5, two methylene signals are observed in all spectra indicating that *n*-butane is distributed over both cages at all loadings. The signal with the largest

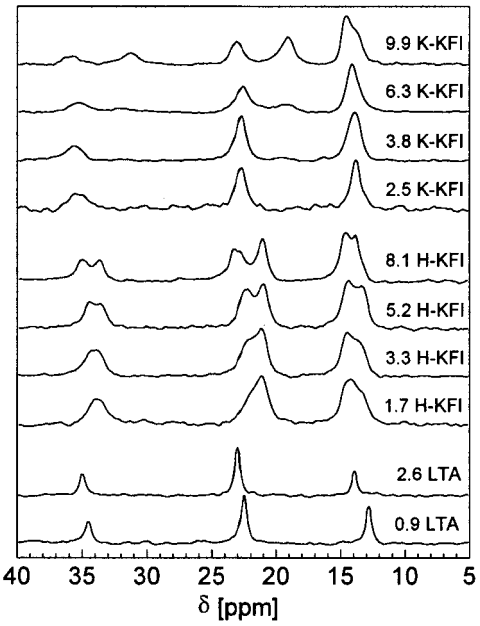

Figure 11. ^{13}C NMR spectra of *n*-pentane in K-ZK-5 (K-KFI), H-ZK-5 (H-KFI), and CaA (LTA) at different loadings, indicated in units of molecules per unit cell.

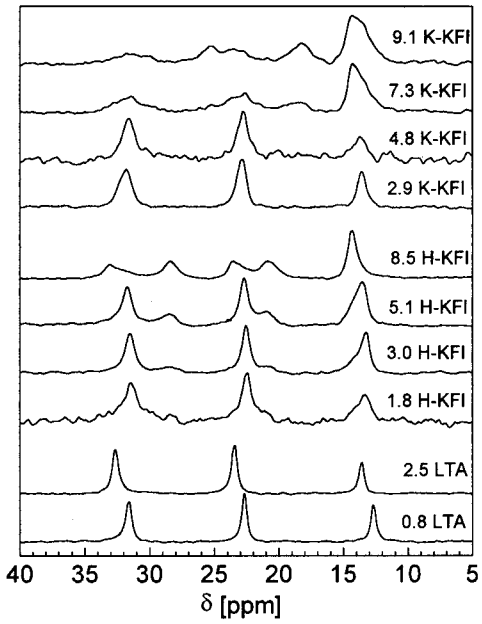

Figure 12. ^{13}C NMR spectra of *n*-hexane in K-ZK-5 (K-KFI), H-ZK-5 (H-KFI), and CaA (LTA) at different loadings, indicated in units of molecules per unit cell.

chemical shift corresponds well with the signals found for CaA and is, thus, assigned to *n*-butane adsorbed in the α-cages. Because, this signal increases in magnitude with loading, adsorption of *n*-butane in the γ-cage is preferred over the α-cage. Only one methyl and one methylene signal is observed for *n*-butane adsorbed in H-ZK-5. The shifts correspond reasonably with those measured for CaA. However, the shifts do not display the same changes with loading as those of *n*-butane in CaA. This would be expected when the *n*-butane molecules are only adsorbed in the α-cages and hence the loading of 6.9 mol/UC would consequently correspond to 3.5 mol/α-cage. Therefore, we assign these signals to *n*-butane adsorbed in the α-cages and γ-cages.

Adsorption of *n*-pentane in H-ZK-5 leads at all loadings to two sets of three signals, corresponding to the three different carbon atoms, indicating simultaneous adsorption in both cages (see Figure 11). The methyl signal with the smallest chemical shift and the C2/C4 methylene signal with the largest chemical shift appear at low loadings only as shoulders and increase in magnitude with increasing loading. Because these latter signals agree well with the signals measured for CaA, they are assigned to *n*-pentane adsorbed in the α-cages. This assignment means that adsorption of *n*-pentane in the γ-cages is preferred under the present conditions. Similar to CaA, an increase in the chemical shift with increasing loading is measured for the signals corresponding to the α-cages of H-ZK-5. Only one set of signals is measured for *n*-pentane adsorbed in K-ZK-5 at low loadings (2.5 and 3.8 mol/UC). On the basis of their chemical shifts, these signals are assigned to *n*-pentane molecules located in the α-cages. This means that, in contrast to H-ZK-5, the α-cages are the preferred adsorption sites of the *n*-pentane molecules. Additional signals appear at higher loadings as a result of adsorption in the γ-cages.

The spectra of *n*-hexane adsorbed in H-ZK-5 show two sets of signals (Figure 12). Although there is some overlap of the two methyl signals, the methylene signals are clearly separated. The signals assigned to hexane in the γ-cages are very weak at the lowest loading and increase in magnitude with increasing loading. This shows that adsorption in the α-cages is preferred, but also that some adsorption in the γ-cages takes place already at a loading of 1.8 mol/UC. Adsorption of *n*-hexane in K-ZK-5 results, up to a loading of 4.8 mol/UC, in one set of signals corresponding to adsorption in the α-cages. Additional methylene signals, assigned to *n*-hexane adsorbed in the γ-cages, occur at higher loadings.

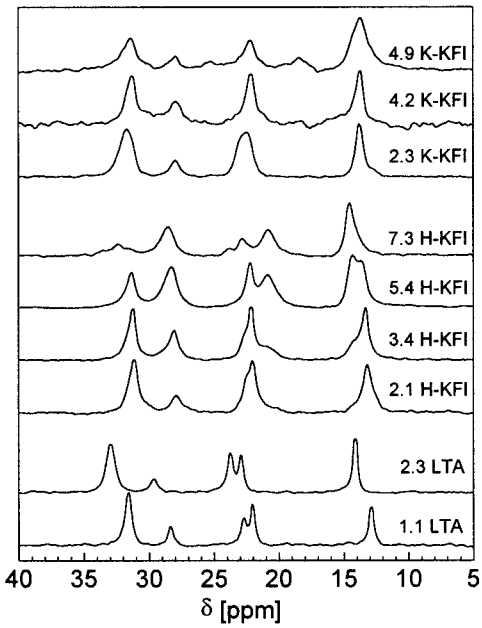

Figure 13. ^{13}C NMR spectra of *n*-heptane in K-ZK-5 (K-KFI), H-ZK-5 (H-KFI), and CaA (LTA) at different loadings, indicated in units of molecules per unit cell.

The spectra obtained from adsorbed *n*-heptane are depicted in Figure 13. The spectra of *n*-heptane adsorbed in CaA show a splitting of the C2/C6 methylene signal which may be due to different degrees of cage filling. It is surprising that a splitting is only observed for this signal. As in liquid *n*-heptane, the central C4 carbon atom yields a signal (approximately 28 ppm) which lies between the signals of the C2/C6 and C3/C5 methylene carbon atoms.[26] The spectra of 2.1, 3.4, and 5.4 mol/UC of *n*-heptane adsorbed in H-ZK-5 display two additional signals at 14.3 and 20.9 ppm that do not correspond with the

signals of *n*-heptane in CaA. Adsorption of *n*-heptane in the α-cages is apparently preferred because these two additional signals are very weak at the lowest loading. Together with the two additional signals, the signal around 28 ppm increases in magnitude with loading. This suggests that this signal is also partly due to *n*-heptane molecules (probably the C3/C5 carbon atom) adsorbed in the γ-cage. The latter is also reasonable because 28 ppm is close to the position of the signal of the C3/C5 carbon atom of *n*-hexane in the γ-cage of H-ZK-5. Adsorption of 2.3 and 4.2 mol/UC of *n*-heptane in K-ZK-5 results in four NMR signals that correspond well with the signals found for CaA. Two weak additional signals occur at 18.7 and 25.1 ppm for a loading of 4.9 mol/UC. These additional signals, together with the pronounced broadening of the methyl signal at 4.9 mol/UC, suggest that some of the adsorbed *n*-heptane molecules are located in the γ-cages of K-ZK-5 at this loading.

The ^{13}C NMR measurements show that the preference for adsorption in the γ-cages decreases with increasing chain length and that significant differences exist between the distributions of the molecules for H-ZK-5 and for K-ZK-5. The γ-cages are the preferred adsorption sites for *n*-alkanes up to *n*-pentane for H-ZK-5 and for molecules up to *n*-butane for K-ZK-5 at room temperature. Although adsorption of *n*-hexane and *n*-heptane in the γ-cages of H-ZK-5 occurs at low loadings, adsorption of *n*-pentane and longer molecules initially and exclusively takes place in the α-cages of K-ZK-5. The observed distributions of the molecules show that the low-temperature desorption peaks of the long molecules are mainly caused by the desorption from the γ-cages. The relatively high pressures required for adsorption of the long molecules are mainly caused by the adsorption in the γ-cages.

The present results show that a change in the number of molecules in an α-cage leads to a change in the chemical shift. The splitting of the C2/C6 signal of *n*-heptane in CaA also suggests that a variation in this loading can result in different, separated signals. This would mean that the C2/C6 signals at 22.1, 22.8−23.0, and 23.8 ppm correspond to 1, 2, and 3 molecules of *n*-heptane per α-cage, respectively. A few examples of adsorption in the α-cages of H-ZK-5 support this interpretation. The spectrum of 8.1 mol/UC of *n*-pentane displays a splitting of the C2/C4 signal; the C2/C5 and C3/C4 signals of 8.5 mol/UC of *n*-hexane in H-ZK-5 are rather asymmetric. The C2/C6 signals of 2.1 and 3.4 mol/UC of *n*-heptane in H-ZK-5 show a shoulder around 22.6 ppm. The latter is almost the same shift as that measured for the C2/C6 signal at higher loadings and might correspond to two *n*-heptane molecules per α-cage. This is in agreement with the assignment of the C2/C6 signals of *n*-heptane in CaA. Finally, the C3/C5 signal of *n*-heptane is split at a loading of 7.3 mol/UC.

3.4.3. Conformational Equilibria of the Molecules. Apart from the distributions of the molecules over the various adsorption sites, the NMR results provide information about the conformational equilibria of the *n*-alkanes at these sites. The spectra of *n*-pentane, *n*-hexane, and *n*-heptane in H-ZK-5 show that the molecules in the γ-cages yield methyl signals at larger chemical shifts and methylene signals at smaller chemical shifts than the molecules in the α-cages. This confirms that the effect of the adsorption environment and that of the conformational equilibrium on the carbon chemical shifts are opposite when molecules adsorbed in the α- and γ-cages are compared. For all *n*-alkanes, it is observed that adsorption in the γ-cages results in smaller methylene chemical shifts. This proves that the molecules in the γ-cages are more coiled (i.e., have a larger contribution of gauche conformations) than those in the α-cages.

TABLE 11: Changes of the ^{13}C NMR Chemical Shifts of Propane to *n*-Heptane in CaA upon an Increase of the Loading (from About 1 to 3 mol/UC); Displayed Results Are Derived from the Data Given in Tables 6−10

alkane	Δ δ (C1)	Δ δ (C2)	Δ δ (C3)	Δ δ (C4)
propane	0.7	0.4		
n-butane	0.9	0.5		
n-pentane	1.1	0.5	0.4	
n-hexane	0.9	0.8	1.0	
n-heptane	1.2	0.9	1.4	1.3

Because of the stronger effect of the medium on the methyl carbons than on the methylene carbons, the effect of the conformational equilibria is compensated by the medium effect for the methyl carbon atoms. This interplay of the two (opposing) effects results in some cases in an overlap of the methyl signals of the molecules in the α- and γ-cages.

The molecules adsorbed in the α-cages of H-ZK-5 and K-ZK-5 yield very similar NMR spectra, indicating that the conformational equilibria of the molecules are alike in these cages. In contrast, adsorption in the γ-cages of K-ZK-5 results in significantly smaller methylene chemical shifts than in the γ-cages of H-ZK-5. This points to a higher degree of coiling of the molecules in the γ-cages of K-ZK-5.

Translation of the differences in chemical shifts of the methylene carbon atoms as a function of chain length to differences in conformational equilibria as a function of chain length should be done carefully. Note that the number of 1,4-gauche interactions in which a methylene carbon atom participates increases with chain length up to a maximum of four.[26] It is, however, clear that the differences between the conformational equilibria of *n*-alkanes in the α- and γ-cages increase with chain length. Moreover, these differences are generally larger for K-ZK-5 than for H-ZK-5.

Finally, a very interesting trend can be seen in the changes of the chemical shifts with loading as a function of the chain length of the molecules adsorbed in the α-cages of CaA. The changes of the carbon chemical shifts upon an increase of the loading in CaA are displayed in Table 11.

The results for propane show that changes in the medium effects contribute to the increases of the chemical shift with loading. The increase of the methylene carbon chemical shift with loading is about half the increase of the methyl carbon chemical shift for propane, *n*-butane, and *n*-pentane. In contrast, the increases of the methylene chemical shifts are as large as or larger than the increase of the methyl chemical shift for *n*-hexane and *n*-heptane. These relatively large increases of the methylene chemical shifts of *n*-hexane and *n*-heptane cannot be explained by the medium effects experienced by the molecules. They are, rather, attributed to changes in conformational equilibria with loading. As noted above, the number of 1,4-gauche interactions in which methylene carbons participate increases with chain length. In contrast, the methyl carbons participate in only one 1,4-gauche interaction in all molecules. Thus, the effect of changes in conformational equilibria becomes stronger for the methylene carbons (especially the inner methylene atoms) with increasing chain length, whereas it remains constant for the methyl carbon atoms. The observed relatively large increases of the methylene chemical shift of *n*-hexane and *n*-heptane indicate that the contribution of trans conformations increases upon an increase of the number of molecules in the α-cages.

3.5. Simulation Results. *3.5.1. Adsorption of Linear Alkanes in KFI.* Adsorption of propane to *n*-heptane in *KFI* was simulated at 298 K using the propane and the Smit et al.

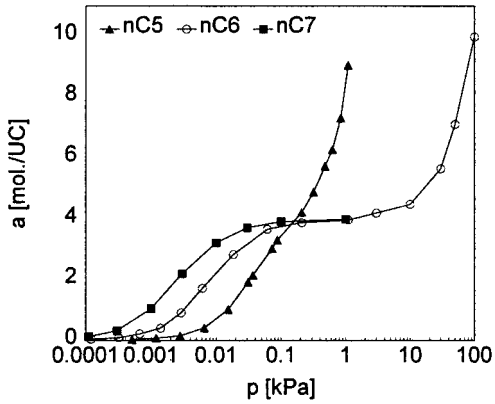

Figure 14. Adsorption isotherms of *n*-pentane, *n*-hexane, and *n*-heptane on KFI at 298 K. The isotherms are calculated with the Smit et al. parameter set.

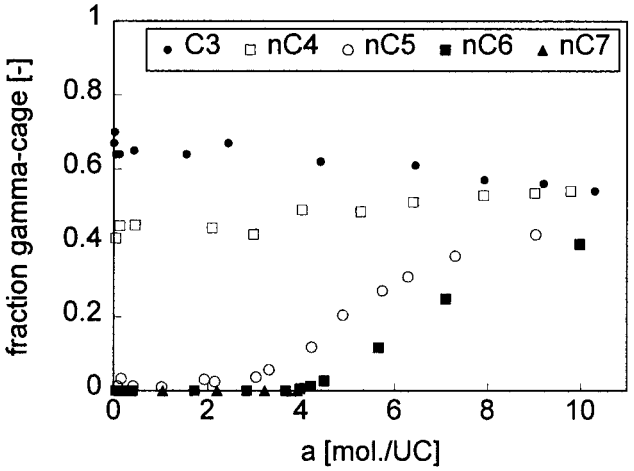

Figure 15. Fraction of adsorbed molecules located in the γ-cages of KFI as a function of loading at 298 K. Results are calculated with the propane (for C3) and Smit et al. (for nC4 and longer) parameter sets.

parameter sets. The adsorption isotherms of *n*-pentane to *n*-heptane are displayed in Figure 14. The loadings of the alkanes are expressed in the number of molecules per unit cell. Because of the difficulty in obtaining higher loadings, the isotherm of *n*-heptane was only simulated up to a loading of 4 mol/UC. In agreement with the experimental isotherms, the number of adsorbed molecules increases with chain length at low loadings and decreases with increasing chain length at high loadings.

The distributions of the alkane molecules over the α- and γ-cages were determined on the configurations obtained from the simulations. The fraction of molecules located in the γ-cages is depicted in Figure 15 as a function of loading. This figure shows that the preference for adsorption in the γ-cages decreases with increasing chain length. The results show furthermore that adsorption of long molecules is limited to the α-cages at low loadings. As illustrated by the isotherms depicted in Figure 14, increased pressures are necessary to adsorb these molecules in the γ-cages.

Figure 16 displays the number of molecules per γ-cage versus the number of molecules per α-cage. The figure shows that the adsorption in the γ-cage is limited to one molecule per cage; the maximum number of molecules in the α-cages is three. For *n*-pentane and *n*-hexane, adsorption in the γ-cage and adsorption of the third molecule in the α-cages occurs simultaneously. Because *n*-hexane displays a step in its adsorption isotherm at 2 mol/α-cage (4 mol/UC), this means that adsorption of the third *n*-hexane molecule in the α-cage results in relatively high

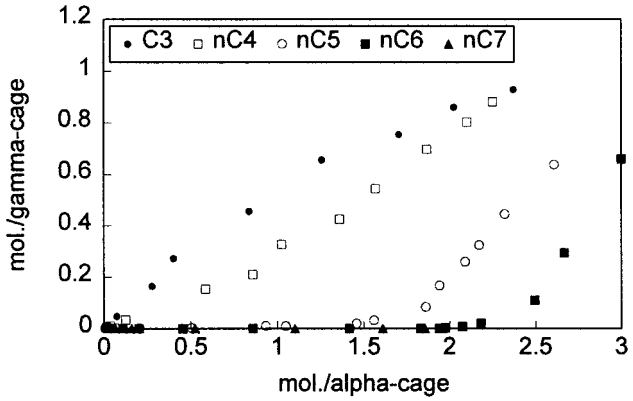

Figure 16. Number of molecules in the γ-cages versus the number of molecules in the α-cages of KFI at 298 K. Results are calculated with the propane (for C3) and Smit et al. (for nC4 and longer) parameter sets.

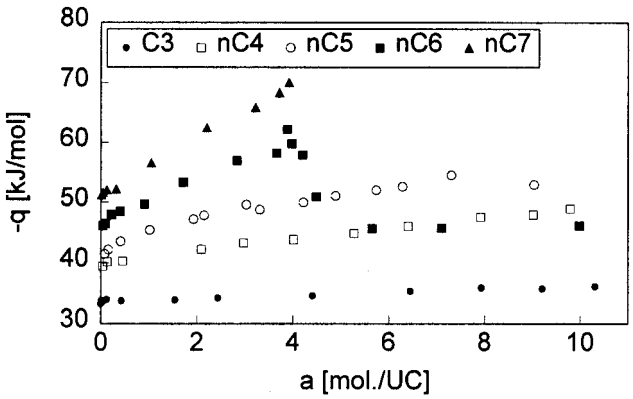

Figure 17. Isosteric heat of adsorption on KFI as a function of loading at 298 K. Results are calculated with the propane (for C3) and Smit et al. (for nC4 and longer) parameter sets.

(or small negative) Gibbs free energies. This is exactly the behavior that is displayed in the TPD results for CaA which show that the third *n*-hexane, *n*-heptane, or *n*-octane molecule per α-cage desorbs at a much lower temperature than the first and second molecule. The above-mentioned observations indicate that desorption of the longer molecules from ZK-5 at relatively low temperatures (or high loadings) may be caused by desorption from the γ-cages and by desorption of the third molecule from the α-cages. The NMR results for H-ZK-5 confirm this conclusion. The NMR spectra show only at high loadings a splitting or an asymmetric shape of the signals assigned to molecules in the α-cages. Because this is caused by adsorption of the third molecule in some of the α-cages, this indicates that adsorption of the third *n*-pentane, *n*-hexane, or *n*-heptane molecule per α-cage takes place only at high loadings.

3.5.2. Comparison of Parameter Sets. The step in the calculated adsorption isotherm of *n*-hexane on *KFI* is in disagreement with the smooth isotherm of *n*-hexane on H-ZK-5 measured experimentally. The calculated isosteric heats of adsorption of propane to *n*-hexane as a function of loading are displayed in Figure 17. The figure shows a decrease in the *n*-hexane heat of adsorption (heat of adsorption becomes less negative) at a loading of 4 mol/UC. This is the same loading at which the step in the calculated adsorption isotherm occurs. This decrease of the heat of adsorption is in disagreement with the experimental results of Eder et al. on H-ZK-5.[22] These results do not display a decrease in the *n*-hexane heat of adsorption up to a loading of 7.4 mol/UC. Furthermore, the simulations predict

TABLE 12: Fraction of Adsorbed Molecules in the γ-Cages at Low Loadings; Results Are Calculated with the Propane/Smit et al. and June et al. Parameters on the All-Silica KFI Structure

alkane	KFI propane/Smit et al.	KFI June et al.
propane	0.67	0.81
n-butane	0.40	0.85
n-pentane	0.01	0.67
n-hexane	0	0.14
n-heptane	0	0.004

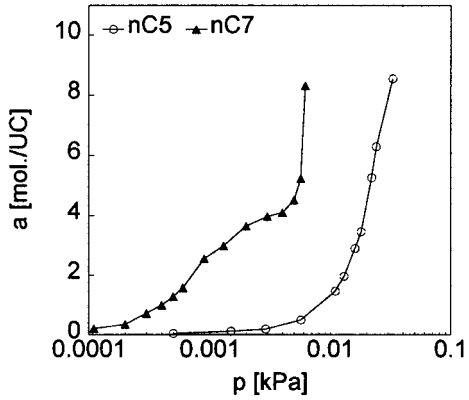

Figure 18. Adsorption isotherms of *n*-pentane and *n*-heptane on KFI at 298 K. The isotherms are calculated with the June et al. parameter set.

that the *n*-pentane and *n*-hexane molecules hardly adsorb in the γ-cages at low loadings. In contrast, the NMR results show that *n*-pentane adsorbs preferentially in the γ-cages and that *n*-hexane is distributed over both cages of H-ZK-5 at low loadings.

The observed discrepancies of the simulated results with the experimental results are probably largely due to the use of a parameter σ that is too large. We showed previously that the size parameter of 3.64 Å of the Smit et al. parameters is too large to obtain a completely correct description of the adsorption properties of alkanes in ferrierite.[8] The use of a too large size parameter leads to an overestimation of the contributions of repulsive interactions to the total interaction between the zeolite framework and the alkane molecules. This is because the calculated interaction between an oxygen atom and an alkane united atom becomes repulsive when the distance between them is less than the size parameter σ used.

To illustrate our viewpoint, we performed some calculations with the June et al. parameters.[21] This parameter set has a size parameter of 3.364 Å which was shown to be somewhat too small.[8] The fraction of molecules adsorbed in the γ-cages of *KFI* at low loadings as predicted with these parameters are compared to the results obtained with the propane and Smit et al. parameter sets in Table 12. In agreement with the NMR results on H-ZK-5, the June et al. parameters predict that the *n*-pentane molecules prefer the γ-cages and the *n*-hexane and *n*-heptane molecules are at all loadings distributed over the two cages. In contrast to the Smit et al. parameters, no decrease in the heat of adsorption with increasing loading is found for propane to *n*-heptane. The calculated adsorption isotherms of *n*-pentane and *n*-heptane on *KFI* show, however, that the value of 3.364 Å is indeed too small. These isotherms are depicted in Figure 18. Whereas the experimental *n*-pentane and *n*-hexane isotherms on H-ZK-5 cross at a loading of about 3 mol/UC, the calculated isotherms do not cross at all. This relative overestimation of the loading of the long alkanes compared to that of the short alkanes has also been found for *n*-hexane/*n*-butane on ZSM-5 and for *n*-pentane/*n*-butane on ferrierite.[8,16]

TABLE 13: Initial Isosteric Heat of Adsorption of Alkanes; Experimental Values Are Determined on H-KFI;[22] Calculated Values are Determined with the Propane/Smit et al. and the June et al. Parameters on the All-silica KFI Structure

alkane	experimental $-q_{st}$ [kJ/mol]	calc. Smit et al. $-q_{st}$ [kJ/mol]	calc. June et al. $-q_{st}$ [kJ/mol]
propane	50	33	31
n-butane	55	40	41
n-pentane	60	42	47
n-hexane	63	47	46
n-heptane		52	51

TABLE 14: Interaction of Molecules with the Zeolite Oxygen Atoms within a Distance of 13.8 Å Calculated with the Propane/Smit et al. and June et al. Parameters; Interactions Are Given in kJ/mol and Differentiated to Molecules in the α-Cages and in the γ-Cages

	Smit et al.		June et al.	
alkane	α−cage	γ−cage	α−cage	γ−cage
propane	−25	−34	−22	−30
n−butane	−33	−43	−29	−40
n−pentane	−40	−45	−37	−49
n−hexane	−46	−44	−44	−57
n−heptane	−52		−52	−63

The initial isosteric heats of adsorption calculated with the different parameter sets are compared with the experimental results of Eder et al. in Table 13.[22] The differences of about 16 kJ/mol between the calculated and the experimental results are larger than can be explained by the contribution of the acid sites to the experimentally determined heats of adsorption.[27] This shows that the energy parameters of the Lennard−Jones potential also require further optimization. The underestimation of the heat of adsorption leads to an underestimation of the Henry's constant. As a consequence, the calculated isotherms are shifted to higher pressures in comparison with the experimental isotherms on H-ZK-5.

3.5.3. Thermodynamics of the Adsorption Phenomena in ZK-5. The simulation results obtained with the propane/Smit et al. and June et al. parameters will be used here to obtain a better insight into the thermodynamic background of the sorption phenomena found in ZK-5. The interaction of the alkane molecules with the zeolite framework was calculated for this purpose. In this analysis, we used the configurations of the molecules obtained from the simulations and calculated their interactions with the framework oxygen atoms that are within the cut-off distance of 13.8 Å. This means that only the tail correction was neglected. The results are differentiated to molecules in the α-cages and γ-cages and are displayed in Table 14.

The influence of the size parameters is clearly reflected in these results. The simulations performed with the June et al. parameters predict that the enthalpic interaction with the framework is for all molecules (from propane to *n*-heptane) more favorable in the γ-cages than in the α-cages. The use of the propane/Smit et al. parameters leads to such a prediction only for propane, *n*-butane, and *n*-pentane. The less favorable enthalpic interaction for *n*-hexane in the γ-cages is the cause of the decrease, incorrectly predicted, in the total heat of adsorption of *n*-hexane (see Figure 17).

A combination of the above results with the distributions of the molecules given in Table 12 reveals that the longer molecules adsorb preferentially in the α-cages despite their more favorable enthalpic interaction with the zeolite framework (and more favorable heat of adsorption) in the γ-cages. This has to mean that the distribution of the longer molecules is determined

TABLE 15: Fraction of Gauche Conformers Calculated with the Smit et al. and June et al. Parameters; Results are Differentiated to Molecules in the α-Cages and in the γ-Cages of KFI

	Smit et al.		June et al.	
n-alkane	α−cage	γ−cage	α−cage	γ−cage
n-butane	0.34	0.61	0.39	0.47
n-pentane	0.33	0.62	0.32	0.45
n-hexane	0.42	0.78	0.39	0.59
n-heptane	0.47		0.42	0.63

by the smaller loss of entropy upon adsorption in the large α-cages than in the small γ-cages. In contrast, adsorption of the smaller molecules occurs preferentially in the γ-cages as a result of the more favorable enthalpic interaction with the framework and despite the larger loss of entropy. The smaller loss of entropy upon adsorption in the α-cages was confirmed by several simulations at 348 K. These simulations show that the fraction of molecules located in the γ-cages at low loadings decreases with increasing temperature.

The enthalpic interactions of the alkane molecules in the α-cages with the zeolite framework given in Table 14 are hardly dependent on the loading. This means that the relatively high pressure required for adsorption of the third long molecule in the α-cages is caused by a relatively large loss of entropy. Note that Peinze et al. reported a distinct increase of the loss of entropy upon an increase of the loading from 1 to 2 molecules of *n*-decane per α-cage in zeolite A.[28] The TPD results on CaA show that the desorption temperature of the third molecule per α-cage decreases with increasing chain length and indicate, therefore, that this loss of entropy increases strongly with chain length.

The following picture of the adsorption behavior of long *n*-alkane (*n*-hexane and longer) molecules can be drawn from the simulations. Long *n*-alkane molecules adsorb initially mainly in the α-cages. Because the loss of entropy is relatively small, the adsorption behavior is determined by the gain in enthalpy upon adsorption in the α-cages. This gain increases with chain length, and therefore, the number of adsorbed molecules increases also with chain length. This behavior is displayed in the simulated and experimental isotherms at low pressures and in the TPD curves at high temperatures. At higher loadings (typically 4 mol/UC or 2 mol/α-cage), adsorption in the γ-cage and adsorption of a third molecule per α-cage becomes significant for long *n*-alkane molecules. Because the loss of entropy is relatively large, the adsorption behavior is determined by the loss of entropy upon adsorption in the α- and γ-cages at higher loadings. This loss increases with chain length, and therefore, the number of adsorbed molecules decreases with increasing chain length. This is displayed in the isotherms at high pressures and in the TPD curves at low temperatures.

3.5.4. Conformational Equilibria. Table 15 displays the fractions of gauche conformers for molecules located in the α-cages and in the γ-cages of *KFI*. The results for *n*-butane to *n*-heptane obtained with the parameters of Smit et al. and the results for *n*-heptane obtained with the June et al. parameters are displayed.

Because of the smaller size parameter, the fractions of gauche conformers predicted with the June et al. parameters are somewhat smaller than those predicted with the Smit et al. parameters. However, the trends in the conformational equilibria are the same for the two parameter sets. In agreement with the NMR results, the calculated fraction of gauche conformers is larger for molecules in the γ-cages than for the molecules in the α-cages. The fractions of gauche conformers for *n*-alkanes

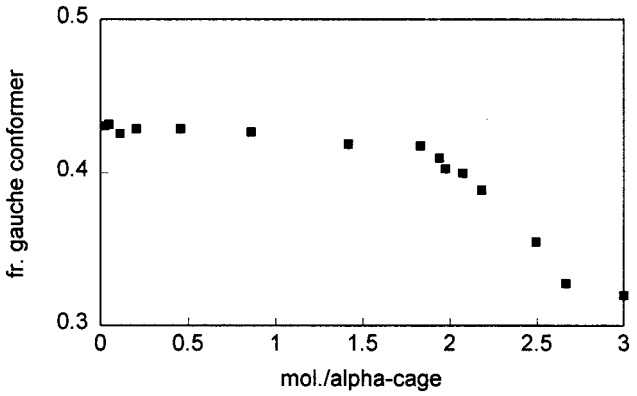

Figure 19. Fraction of gauche conformers of *n*-hexane molecules in the α-cages as a function of the number of molecules in the α-cage at 298 K. Results are calculated with the Smit et al. parameter set.

in the α-cages of *KFI* agree well with previously calculated conformational equilibria of *n*-alkanes in the α-cages of zeolite A and with the calculated conformational equilibrium of *n*-butane in NaCaA.[24,29]

The results for the molecules in the α-cages given in Table 15 are obtained for loadings below 2 mol/α-cage. Above this loading, a significant decrease of the fraction of gauche conformers occurs. A typical example is depicted in Figure 19 which shows, as a function of number of molecules per α-cage, the fraction of gauche conformers for *n*-hexane molecules in the α-cages as calculated with the Smit et al. parameters. This fraction becomes about a tenth smaller from 2 to 3 mol/α-cage for all alkane molecules. The increased stretching of the molecules with increasing loading might lead to a closer packing of the molecules. The decrease in the fraction of gauche conformers with loading agrees with our NMR results for molecules adsorbed in the α-cages of CaA. The calculated changes in the conformational equilibria give a significant contribution (at least 0.5 ppm) to the observed increases of the chemical shifts with loading. In contrast to our results, Bandyopadhyay and Yashonath calculated an increase of the fraction of *n*-butane gauche conformers from 0.40 to 0.57 upon the increase of the loading from 1 to 5 mol/α-cage of NaCaA.[29]

4. Conclusions

We showed by means of a combination of adsorption, desorption, and ^{13}C NMR measurements and CB−MC simulations that the adsorption properties of *n*-alkane molecules in ZK-5 zeolites are highly dependent on the chain length of the molecule. *n*-Alkanes up to *n*-heptane adsorb in the α- and γ-cages of ZK-5, whereas *n*-octane (and longer) molecules are excluded from adsorption in the small γ-cages and adsorb only in the α-cages.

The γ-cages are the preferred adsorption sites of the short alkane molecules because of the more favorable heat of adsorption and despite the lower entropy in these cages. In contrast, the longer molecules adsorb preferentially in the large α-cages as a result of the higher entropy and despite the less favorable heat of adsorption in these cages. This difference in siting is the result of a very steep decrease of the entropy of the molecules in the γ-cages with increasing chain length. As a result of the large loss of entropy, adsorption of *n*-pentane and longer molecules in the γ-cages is determined by the loss of entropy. This means that the pressure that is required for adsorption in the γ-cages increases with increasing chain length. The entropy of the long alkane molecules is distinctly smaller in the γ-cages than in the α-cages and these molecules display,

therefore, two-stage desorption profiles and steps in their adsorption isotherms.

Adsorption into the large α-cages is determined by the gain in enthalpy at low loading. Consequently, the number of adsorbed molecules increases with chain length. Adsorption of a third *n*-hexane or longer molecule in the α-cages leads to, in comparison to adsorption of the first two molecules, a large loss of entropy. As a result, adsorption of the third long alkane molecule into the α-cages is determined by the loss of entropy and occurs at relatively high pressures.

The adsorption properties of alkanes in H-ZK-5 and K-ZK-5 are significantly different. The molecules adsorbed in the γ-cages of K-ZK-5 are in a much more constrained position than those in the γ-cages of H-ZK-5. This is due to the presence of potassium extra-framework cation in the γ-cages of K-ZK-5. *n*-Heptane molecules are adsorbed easily in the γ-cages of H-ZK-5, whereas they hardly adsorb in the γ-cages of K-ZK-5. *n*-Pentane adsorbs, at room temperature, preferentially in the γ-cages of H-ZK-5, whereas it adsorbs preferentially in the α-cages of K-ZK-5.

The ^{13}C NMR investigations and the simulation results on the conformational equilibria of the adsorbed *n*-alkane molecules are in good agreement. The molecules adsorbed in the γ-cages are in general more coiled (larger contribution of gauche conformers) than those adsorbed in the α-cages. The conformational equilibria of the molecules in the α-cages of H-ZK-5 and of K-ZK-5 are comparable. However, the molecules in the γ-cages of K-ZK-5 have significantly more gauche conformers than those in the γ-cages of H-ZK-5. An increase of the number of molecules in the α-cages from two to three results in a decrease of the contribution of gauche conformers.

The comparison between the simulation results obtained with different parameter sets and the experimental results confirms our previous conclusion that a size parameter between 3.364 and 3.64 Å is required for a correct description of the adsorption behavior of *n*-alkanes in zeolites. The results also indicate that the used energy parameters underestimate the heats of adsorption and Henry's constants for adsorption of *n*-alkanes in zeolite ZK-5.

Acknowledgment. We thank Berend Smit for providing the simulation programs and for useful discussions. Xavier Cottin is acknowledged for his support regarding the molecular simulations. E. I. DuPont de Nemours and Exxon Chemical Europe Inc. are acknowledged for the supply of the NH_4-ZK-5 and K-ZK-5 samples. W. J. M. van Well is financially supported by the Dutch Organization for Scientific Research (NWO) through the Netherlands Research Council for Chemical Sciences.

References and Notes

(1) Initial results will be published as: Jänchen, J.; van Well, W. J. M.; van Wolput, J. H. M. C.; Stach, H. *Proceedings of the 12th International Zeolite Conference*, Baltimore, 1998.
(2) Smit, B.; Maesen, T. L. M. *Nature* **1995**, *374*, 42.
(3) Van Well, W. J. M.; Wolthuizen, J. P.; Smit, B.; van Hooff, J. H. C.; van Santen, R. A. *Angew. Chem., Int. Ed. Engl.* **1995**, *34*, 2543.
(4) Olson, D. H.; Reischman, P. T. *Zeolites* **1996**, *17*, 434.
(5) Smit, B.; Siepmann, J. I. *Science* **1994**, *264*, 1118.
(6) Van Well, W. J. M.; Cottin, X.; de Haan, J. W.; van Santen, R. A.; Smit, B. *Angew. Chem., Int. Ed. Engl.* **1998**, *37*, 1081.
(7) Van Well, W. J. M.; Cottin, X.; de Haan, J. W.; van Hooff, J. H. C.; van Santen, R. A.; Smit, B.; Nivarthy, G.; Lercher, J. A. *J. Phys. Chem. B.* **1998**, *102*, 3945.
(8) Van Well, W. J. M.; Cottin, X.; van Hooff, J. H. C.; van Santen, R. A.; Smit, B. *J. Phys. Chem. B.* **1998**, *102*, 3952.
(9) Bates, S. P.; van Well, W. J. M.; van Santen, R. A.; Smit, B. *J. Am. Chem. Soc.* **1996**, *118*, 6753.
(10) Kerr, G. T. *Science* **1966**, *140*, 1412.
(11) Barrer, R. M. *J. Chem. Soc.* **1948**, 127.
(12) Abrams, L.; Corbin, D. R. *J. Inclusion Phenom. Mol. Recognit. Chem.* **1995**, *21*, 1.
(13) Lievens, J. L.; Verduijn, J. P.; Mortier, W. J. *Zeolites* **1992**, *12*, 690.
(14) Parise, J. B.; Shannon, R. D.; Prince, E.; Cox, D. E. *Z. Kristallogr.* **1983**, *165*, 175.
(15) Smit, B.; Siepmann, J. I. *J. Phys. Chem.* **1994**, *98*, 8442.
(16) Smit, B. *Mol. Phys.* **1995**, *85*, 153.
(17) Frenkel, D.; Smit, B. *Understanding molecular simulations: from algorithms to applications*; Academic Press: San Diego, 1996.
(18) Vlugt, T. J. H.; Martin, M. G.; Smit, B.; Siepmann, J. I.; Krishna, R. *Mol. Phys.* **1998**, *94*, 727.
(19) http://molsim.chem.uva.nl/bigmac.
(20) Smit, B. *J. Phys. Chem.* **1995**, *99*, 5597.
(21) June, R. L.; Bell, A. T.; Theodorou, D. N. *J. Phys. Chem.* **1992**, *96*, 1051.
(22) Eder, F.; Lercher, J. A. *J. Phys. Chem. B* **1997**, *101*, 1273.
(23) Hayashi, S.; Suzuki, K.; Shin, S.; Hayamizu, K.; Yamamoto, O. *Chem. Phys. Lett.* **1985**, *113*, 368.
(24) Bates, S. P.; van Well, W. J. M.; van Santen, R. A.; Smit, B. *J. Phys. Chem.* **1996**, *100*, 17573.
(25) Tonelli, A. E. *NMR spectroscopy and polymer microstructure. The conformational connection*; VCH Publishers: Cambridge, 1989.
(26) Van de Ven, L. J. M.; de Haan, J. W.; Bučinská, A. *J. Phys. Chem.* **1982**, *86*, 2516.
(27) Eder, F.; Lercher J. A. *Zeolites* **1997**, *18*, 75.
(28) Peize, T.; Stach, H.; Fiedler, K.; Schirmer, W. *Chem. Techn.* **1979**, *31*, 306.
(29) Bandyopadhyay, S.; Yashonath, S. *J. Phys. Chem. B* **1997**, *101*, 5675.